tvst

https://doi.org/10.1167/tvst.8.6.26

Article

OCTA-Based Identification of Different Vascular Patterns in Stargardt Disease

Alessandro Arrigo[1], Francesco Romano[1,2], Emanuela Aragona[1], Carlo di Nunzio[1], Andrea Sperti[1], Francesco Bandello[1], and Maurizio Battaglia Parodi[1]

[1] Department of Ophthalmology, IRCCS Ospedale San Raffaele, University Vita-Salute, Milan, Italy
[2] Eye Clinic, Department of Biomedical and Clinical Science, Luigi Sacco University Hospital, Milan, Italy

Correspondence: Alessandro Arrigo, Department of Ophthalmology, IRCCS Ospedale San Raffaele, University Vita-Salute, via Olgettina 60, Milan, 20132, Italy. e-mail: alessandro.arrigo@hotmail.com

Received: 23 May 2019
Accepted: 2 October 2019
Published: 5 December 2019

Keywords: Stargardt disease; OCT; OCTA; vessel density; vessel tortuosity; vessel dispersion; vessel rarefaction

Citation: Arrigo A, Romano F, Aragona E, di Nunzio C, Sperti A, Bandello F, Battaglia Parodi M. OCTA-based identification of different vascular patterns in Stargardt disease. Trans Vis Sci Tech. 2019;8(6):26, https://doi.org/10.1167/tvst.8.6.26

Purpose: The aim of the present study was to analyze quantitative optical coherence tomography (OCT) and OCT angiography (OCTA) parameters to identify clinically relevant cutoff values able to detect clinically different Stargardt's disease (STGD) subgroups.

Methods: Consecutive STGD patients were recruited and underwent complete ophthalmologic examination, including multimodal imaging. Several quantitative parameters were extracted both from structural OCT and OCTA images and were statistically analyzed. A post hoc analysis was performed to identify a quantitative cutoff able to distinguish two clinically different STGD subgroups. Main outcome measures were total retinal thickness, central macular thickness (CMT), retinal layers thickness, retinal and choroidal hyperreflective foci (HF) number, vessel density (VD), vessel tortuosity (VT), vessel dispersion (Vdisp), and vessel rarefaction (VR) of macular and optic nerve head plexa.

Results: Overall, 54 eyes of 54 STGD patients (18 males) and 54 eyes of 54 healthy age- and sex-matched controls were included in the analysis. All quantitative parameters resulted significantly worse in STGD than controls ($P < 0.01$). Moreover, a VT cutoff of 5 allowed to distinguish the following two categories: a functionally and anatomically better STGD group and a worse group. BCVA resulted 0.42 $\pm$ 0.28 logMAR in the best group versus 1.09 $\pm$ 0.36 logMAR in the worst ($P < 0.01$). Structural OCT and OCTA parameters significantly differed between the two STGD groups.

Conclusions: Quantitative OCTA was able to detect different morphofunctional STGD phenotypes.

Translational Relevance: OCTA-based classification of STGD patients detected different patients' subgroups, differing in terms of morphologic and functional features, with a potential impact on clinical and research settings.

Introduction

Stargardt's disease (STGD) is a common hereditary retinal dystrophy leading to irreversible bilateral visual acuity loss.[1] It is characterized by a diffusely compromised retinal pigmented epithelium (RPE)/photoreceptor complex, with heterogeneous manifestations detectable both at the macular level and in the middle and extreme periphery.[2,3] Recently developed noninvasive imaging technology, principally optical coherence tomography (OCT) and OCT angiography (OCTA), has led to a better understanding of the underlying pathologic mechanisms governing the onset and progression of the atrophic process, revealing a connection with the damage to the retinal and choroidal vascular network.[4–6]

The aim of the present study was to analyze quantitative OCTA parameters in order to identify clinically relevant cutoff values.

Materials and Methods

The study was designed as an observational cross-sectional analysis. Consecutive patients affected by

STGD were recruited in the Heredodystrophies Unit of the Department of Ophthalmology of San Raffaele Hospital in Milan. Each patient provided signed informed consent before the examination, in accordance with the Declaration of Helsinki. The study was approved by the Ethical Committee of the Vita-Salute San Raffaele University of Milan. The inclusion criteria were as follows: *ABCA4* genetically confirmed diagnosis of STGD and age from 18 to 70 years. The following exclusion criteria were applied: refractive errors greater than ±3 diopters (D), increased media opacity, glaucoma and other types of retinal and/or optic nerve diseases (e.g., diabetic retinopathy), any ophthalmic surgery in the last 6 months, any systemic conditions potentially affecting the results of the study.

All the patients underwent a complete ophthalmologic examination, including best-corrected visual acuity (BCVA) using standard Early Treatment Diabetic Retinopathy Study charts, slit-lamp evaluation of anterior and posterior segments, intraocular pressure measurement with a Goldmann applanation tonometer, color fundus photography, and fundus autofluorescence. In addition, structural OCT and OCTA images were acquired by means of Heidelberg Spectralis HRA+OCT (Heidelberg Engineering, Heidelberg, Germany) and SS-OCT DRI Topcon Triton (Topcon Corporation, Tokyo, Japan), respectively. The OCT acquisition protocol included high-resolution radial and raster scans, while OCTA analysis included 3 × 3- and 4.5 × 4.5-mm scans, centered at the level of both the macula and the optic nerve head. Eye tracking was used to assess possible fixation loss. Only high-quality images, evaluated by means of Topcon index quality (>70), were considered.

We measured retinal layer thickness by means of a high-resolution horizontal structural enhanced-depth imaging (EDI)-OCT scan,[7] including total retinal thickness, central macular thickness (CMT), retinal nerve fiber layer (RNFL), ganglion cell layer (GCL), inner plexiform layer (IPL), inner nuclear layer (INL), outer plexiform layer (OPL), outer nuclear layer (ONL) and ellipsoid zone–retinal pigment epithelium layer (EZ-RPE). Choroidal thickness was also measured. For each measure, four samplings were obtained on the left and four on the right of the foveal, the mean value being used in the analysis. Moreover, hyperreflective foci (HF) (defined as discrete, punctiform, hyperreflective lesions) were measured in the same structural OCT scan, within both the retina and the choroid, but using inverted colors to improve the imaging. HF were analyzed in a region selected on a horizontal structural OCT, including 750 μm on the right and left sides of a vertical line passing through the fovea. Fundus autofluorescence (FAF) images were also used to assess the presence of foveal sparing, defined as the absence of autofluorescence surrounding the fovea by least 180°, not including the fovea.[8] A control group of healthy age- and sex-matched subjects underwent the same ophthalmologic assessment.

OCTA images were analyzed by the Topcon full-spectrum, amplitude-decorrelation, angiography algorithm. Each patient contributed with a single eye, which was randomly selected.

The superficial capillary plexuses (SCP), deep capillary plexuses (DCP), and choriocapillaris (CC) were automatically segmented both in the macula and in the optic nerve head; additionally, the radial peripapillary capillary (RPC) plexus was automatically segmented at the level of the optic nerve. For convenience, macular parameters will henceforth be referred to using the prefix "m," with the prefix "n" applying to the optic nerve head (e.g., mSCP and nSCP for macular and nerve superficial capillary plexuses, respectively).

Each reconstruction was carefully inspected by an expert ophthalmologist (MBP). All reconstructions were exported in .tiff format and loaded in ImageJ software (Bethesda, MD). In-house scripts were built in order to calculate the following parameters: vessel density (VD), vessel tortuosity (VT), vessel dispersion (Vdisp), and vessel rarefaction (VR), with the same approach already adopted.[9]

The statistical analysis of the quantitative parameters considered, comparing with control values, was performed using the one-way ANOVA test, with Bonferroni correction for multiple comparisons (SPSS, Chicago, IL). Moreover, statistically significant correlations between all considered parameters were assessed by means of Kendall's tau correlation coefficient measurement. We also performed a receiver operating curve (ROC) analysis in order to extract a parameter that could distinguish STGD subgroups differing significantly in terms of BCVA. The statistical significance was set at $P < 0.05$.

Results

Overall, 54 eyes of 54 STGD patients (18 males) were included in the analysis, and all data were compared with 54 eyes of 54 healthy age- and sex-matched controls. All clinical and imaging findings

Table 1. Clinical and Imaging Findings

	STGD Patients		Controls		
Parameter	Mean	SD	Mean	SD	*P* Value
Age	43.52	16.39	45.37	17.93	$P > 0.05$
BCVA, logMAR	0.68	0.44	0.00	0.00	$P < 0.01$
RNFL	97.86	9.45	106.53	9.63	
EZ-RPE	43.87	21.37	73.01	5.55	
ONL	26.19	14.10	92.34	7.25	
OPL	20.12	9.90	41.51	5.98	
INL	33.15	7.71	46.17	6.46	
IPL	34.84	8.85	48.21	7.12	
GCL	44.21	11.21	62.49	7.48	
CMT	103.05	59.03	241.03	11.16	
Retinal thickness	224.23	54.24	400.66	19.06	
Choroidal thickness	257.01	94.71	322.53	44.37	
HF_retina	7.76	7.35	0.00	0.00	
HF_choroid	18.26	17.86	0.00	0.00	
VD mSCP	0.40	0.02	0.41	0.01	
VD mDCP	0.26	0.06	0.43	0.01	
VD mCC	0.32	0.16	0.50	0.01	
VDisp mSCP	24.62	8.72	10.72	4.15	
VDisp mDCP	27.51	8.75	11.45	3.48	
VT mSCP	5.31	0.15	7.20	0.31	
VT mDCP	4.80	0.50	7.84	0.34	
VR mSCP	0.44	0.03	0.39	0.01	
VR mDCP	0.47	0.03	0.41	0.01	
VD RPC	0.42	0.02	0.44	0.01	
VD nSCP	0.41	0.03	0.43	0.01	
VD nDCP	0.30	0.02	0.40	0.02	
VD nCC	0.51	0.03	0.54	0.03	
VDisp RPC	24.78	8.82	10.61	3.70	
VDisp nSCP	25.80	11.56	10.35	2.88	
VDisp nDCP	27.43	9.72	10.37	3.36	
VT RPC	5.64	0.51	7.73	0.30	
VT nSCP	4.45	0.26	8.42	0.33	
VT nDCP	5.20	0.27	7.06	0.25	
VR RPC	0.47	0.02	0.45	0.01	
VR nSCP	0.49	0.02	0.44	0.01	
VR nDCP	0.43	0.02	0.40	0.01	

are extensively reported in Table 1. Duration of STGD, as assessed on the patients' report, was 12.8 ± 10.8 years. The standout finding was STGD patients showed statistically significant worse BCVA, structural OCT parameters, and OCTA parameters. Moreover, we detected significantly higher HF numbers, both within the retina and the choroid in our patients' cohort, with respect to the control group. Partial or complete foveal sparing was detected in 23 of 54 patients (43%). Correlation analyses revealed several statistically significant correlations (Table 2). In more detail, BCVA was influenced by the integrity both of the retinal layers and vascular network. The presence of HF was found to correlate with worse BCVA. Furthermore, both retinal layer thickness and HF number significantly correlated with OCTA parameters. In particular, high VD and VT values were associated with better structural features and lower HF number, whereas high VDisp and VR values were related to worse retinal status and higher HF number. It is worth noting the higher significant correlations with both VD and VT, compared with VDisp and VR parameters. Statistically significant correlations were found when considering macular OCTA parameters alone, optic nerve head parameters showing unremarkable effects (Figs. 1 and 2). Interestingly, retinal layer thickness showed a stronger correlation with VT values than with VD. In addition, as expected, OCTA parameters showed statistically significant correlations between them ($P < 0.01$). No significant age or duration effect were detected. ROC analysis established a cutoff value based on the VT mean, to separate two subgroups with different BCVA, with both sensitivity and specificity of 0.9. A VT cutoff of 5 created two categories, a functionally and anatomically better STGD group (STGD1) and a worse group (STGD2) (Table 3). Foveal sparing was present in 15 of 35 patients of STGD1 (43%) and in 8 of 19 patients of STGD2 (42%) ($P > 0.05$), showing no effects on the analyses.

Discussion

STGD is a complex disease primarily associated with RPE/photoreceptor dysfunction and is accompanied by a compromised vascular network, which can be noninvasively analyzed by OCTA.[6] In particular, macular CC alterations represent a key element contributing to outer retinal atrophy.[4]

The aim of the present study was to analyze both retinal layer and vascular network changes in STGD. A significant thinning of inner and outer retinal layers, together with the presence of relevant alterations of the retinal vascular network were found, providing further confirmation of the CC macular damage. Although significant dysfunction

Table 2. Correlation Analysis

Parameter	RNFL	EZ−RPE	ONL	INL	IPL	GCL	CMT	Full_Retina
BCVA logMAR								
Kendall's tau coefficient	−0.248	−0.939	−0.938	−0.939	−0.941	−0.94	−0.938	−0.938
P value	<0.01	<0.01	<0.01	<0.01	<0.01	<0.01	<0.01	<0.01
	ONL	INL	IPL	GCL	CMT	Full_retina	HF_retina	HF_choroid
EZ-RPE								
Kendall's tau coefficient	0.996	0.995	0.993	0.994	0.998	0.998	−0.548	−0.658
P value	<0.01	<0.01	<0.01	<0.01	<0.01	<0.01	<0.01	<0.01
	INL	IPL	GCL	CMT	Full_retina	HF_retina	HF_choroid	VD mCC
ONL								
Kendall's tau coefficient	0.994	0.994	0.993	0.996	0.997	−0.545	−0.66	0.963
P value	<0.01	<0.01	<0.01	<0.01	<0.01	<0.01	<0.01	<0.01
	IPL	GCL	CMT	Full_retina	HF_retina	HF_choroid	VD mCC	VT mSCP
INL								
Kendall's tau coefficient	0.992	0.993	0.995	0.996	−0.551	−0.661	0.962	0.99
P value	<0.01	<0.01	<0.01	<0.01	<0.01	<0.01	<0.01	<0.01
	GCL	CMT	Full_retina	HF_retina	HF_choroid	VD mCC	VT mSCP	VT mDCP
IPL								
Kendall's tau coefficient	0.991	0.993	0.994	−0.545	−0.663	0.959	0.987	0.992
P value	<0.01	<0.01	<0.01	<0.01	<0.01	<0.01	<0.01	<0.01
	CMT	Full_retina	HF_retina	HF_choroid	VD mCC	VT mSCP	VT mDCP	VT RPC
GCL								
Kendall's tau coefficient	0.994	0.994	−0.548	−0.662	0.961	0.989	0.993	0.993
P value	<0.01	<0.01	<0.01	<0.01	<0.01	<0.01	<0.01	<0.01
	Full_retina	HF_retina	HF_choroid	VD mCC	VT mSCP	VT mDCP	VT RPC	VR mSCP
CMT								
Kendall's tau coefficient	0.998	−0.546	−0.658	0.964	0.991	0.996	0.995	−0.951
P value	<0.01	<0.01	<0.01	<0.01	<0.01	<0.01	<0.01	<0.01
	HF_retina	HF_choroid	VD mCC	VT mSCP	VT mDCP	VT RPC	VR mSCP	VR mDCP
Full_retina								
Kendall's tau coefficient	−0.547	−0.658	0.965	0.991	0.998	0.997	−0.951	−0.961
P value	<0.01	<0.01	<0.01	<0.01	<0.01	<0.01	<0.01	<0.01
	HF_choroid	VD mCC	VT mSCP	VT mDCP	VT RPC	VR mSCP	VR mDCP	VR RPC
HF_retina								
Kendall's tau coefficient	0.665	−0.516	−0.554	−0.547	−0.547	0.535	0.549	0.526
P value	<0.01	<0.01	<0.01	<0.01	<0.01	<0.01	<0.01	<0.01
	VD mCC	VT mSCP	VT mDCP	VT RPC	VR mSCP	VR mDCP	VR RPC	
HF_choroid								
Kendall's tau coefficient	−0.625	−0.657	−0.657	−0.657	0.628	0.663	0.679	
P value	<0.01	<0.01	<0.01	<0.01	<0.01	<0.01	<0.01	

of the optic nerve head plexa was detected, these changes may be interpreted as a consequence of modifications to the retina. Quantitative OCTA parameters, including VT, VDisp, and VR, enabled the involvement of the retinal vascular network in STGD to be described in greater detail. In particular, retinal plexa appeared rarer and more disorganized than in controls, VT reduction representing the consequence of reduced blood flow perfusion.[9]

The dysfunction present throughout the retinal vascular network may be due to the primary RPE/photoreceptor damage. Indeed, the RPE is essential to the physiologic release of growth factors, including VEGF, which guarantee the trophism of retinal

Table 2. Extended

Parameter	HF_retina	HF_choroid	VD mCC	VD nCC	VT mSCP	VT mDCP	VT RPC	VR mSCP
BCVA logMAR								
Kendall's tau coefficient	0.56	0.697	−0.903	0.366	−0.943	−0.939	−0.938	0.925
P value	<0.01	<0.01	<0.01	<0.01	<0.01	<0.01	<0.01	<0.01
	VD mCC	VT mSCP	VT mDCP	VT RPC	VR mSCP	VR mDCP	VR RPC	VT Mean
EZ-RPE								
Kendall's tau coefficient	0.964	0.992	0.997	0.995	−0.952	−0.962	−0.913	0.735
P value	<0.01	<0.01	<0.01	<0.01	<0.01	<0.01	<0.01	<0.01
	VT mSCP	VT mDCP	VT RPC	VR mSCP	VR mDCP	VR RPC	VT Mean	VR Mean
ONL								
Kendall's tau coefficient	0.991	0.997	0.997	−0.951	−0.963	−0.913	0.735	−0.725
P value	<0.01	<0.01	<0.01	<0.01	<0.01	<0.01	<0.01	<0.01
	VT mDCP	VT RPC	VR mSCP	VR mDCP	VR RPC	VT Mean	VR Mean	
INL								
Kendall's tau coefficient	0.995	0.993	−0.952	−0.961	−0.914	0.736	−0.726	
P value	<0.01	<0.01	<0.01	<0.01	<0.01	<0.01	<0.01	
	VT RPC	VR mSCP	VR mDCP	VR RPC	VT Mean	VR Mean		
IPL								
Kendall's tau coefficient	0.993	−0.953	−0.961	−0.918	0.738	−0.726		
P value	<0.01	<0.01	<0.01	<0.01	<0.01	<0.01		
	VR mSCP	VR mDCP	VR RPC	VT Mean	VR Mean			
GCL								
Kendall's tau coefficient	−0.952	−0.962	−0.917	0.731	−0.729			
P value	<0.01	<0.01	<0.01	<0.01	<0.01			
	VR mDCP	VR RPC	VT Mean	VR Mean				
CMT								
Kendall's tau coefficient	−0.962	−0.914	0.735	−0.724				
P value	<0.01	<0.01	<0.01	<0.01				
	VR RPC	VD Mean	VT Mean	VR Mean				
Full_retina								
Kendall's tau coefficient	−0.913	0.373	0.738	−0.724				
P value	<0.01	<0.01	<0.01	<0.01				
HF_retina								
Kendall's tau coefficient								
P value								
HF_choroid								
Kendall's tau coefficient								
P value								

vessels and CC, along with the regulation of metabolic exchanges through the blood–retinal barrier (Le YZ, et al. *IOVS*. 2008;49:E–Abstract 857).[10] With regard to inner retinal thinning, this finding might be explained as inner retinal cell damage caused by anterograde degeneration, taking into account the exclusive expression of the *ABCA4* gene in the RPE/photoreceptor complex.[11] Alternatively, the loss of trophic stimuli from RPE cells, in addition to the retinal vascular network deficiency, may contribute to inner retinal degeneration and thinning. The results of the correlation analysis, especially the strong correlation revealed between retinal layer thickness and VT, further underline the influence of the impaired blood

Table 2. Extended

Parameter	VR mDCP	VR RPC	VD Mean	VT Mean	VR Mean
BCVA logMAR					
Kendall's tau coefficient	0.939	0.944	−0.362	−0.76	0.736
P value	<0.01	<0.01	<0.01	<0.01	<0.01
	VR Mean				
EZ-RPE					
Kendall's tau coefficient	−0.723				
P value	<0.01				
ONL					
Kendall's tau coefficient					
P value					
INL					
Kendall's tau coefficient					
P value					
IPL					
Kendall's tau coefficient					
P value					
GCL					
Kendall's tau coefficient					
P value					
CMT					
Kendall's tau coefficient					
P value					
Full_retina					
Kendall's tau coefficient					
P value					
HF_retina					
Kendall's tau coefficient					
P value					
HF_choroid					
Kendall's tau coefficient					
P value					

supply in the progression of the degenerative process occurring in STGD.

The higher number of retinal and choroidal HF in STGD patients has already been described[12] and represents an imaging biomarker of the disease's activity, as reported in other conditions.[13]

The most interesting findings of the present paper are the results of the cutoff analyses of OCTA parameters. A VT cutoff value of 5, obtained from the mean of the values of all retinal plexa, was able to identify two different STGD groups on the basis of the BCVA. These patients' subgroups also differed in terms of retinal layer thickness and OCTA parameters, thus enabling us to divide our

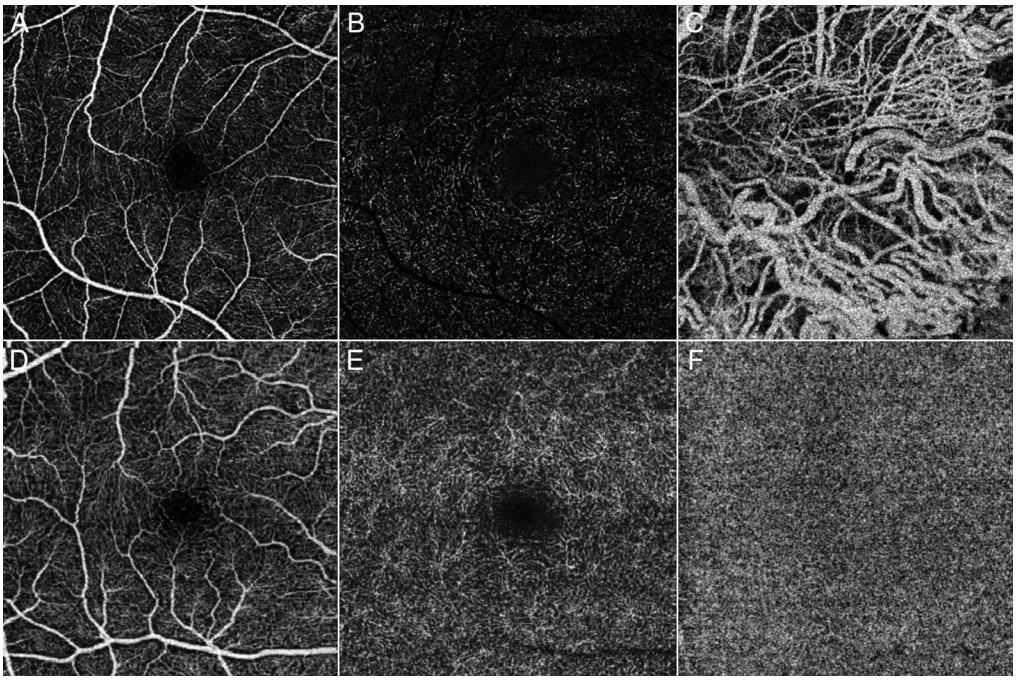

Figure 1. Macular OCTA in STGD. SCP (A) and DCP (B) appear evidently rarefied in STGD. Furthermore, CC (C) results almost absent, with clear exposure of choroidal vessels. SCP, DCP, and CC plexa of a healthy control are shown in (D–F), respectively.

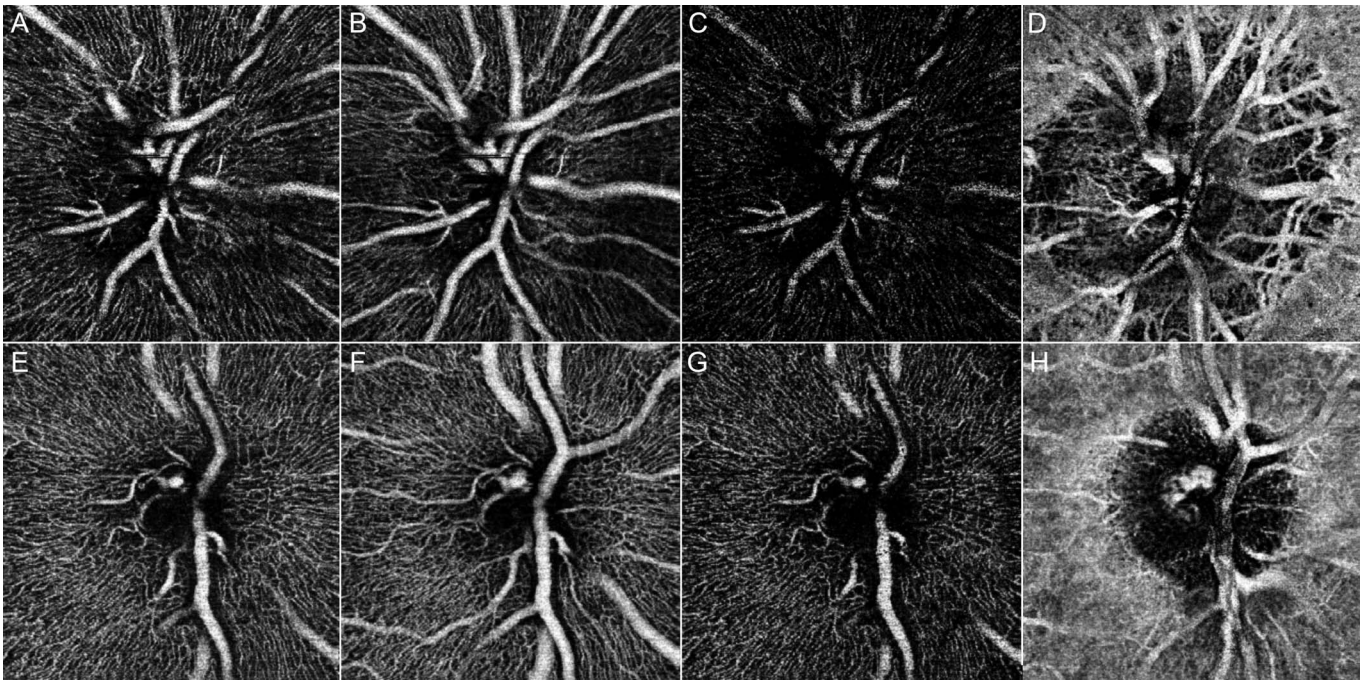

Figure 2. Optic nerve head OCTA in STGD. If comparing a STGD patient with a healthy control, RPC (A), SCP (B), and DCP (C) appear evidently rarefied in STGD. Moreover, also CC plexus shows signs of perfusion lacks (D). RPC, SCP, DCP, and CC plexa of a healthy control are shown in (E–H), respectively.

Table 3. OCTA VT Cutoff Analysis (VT = 5)

Parameter	Mean ± SD	Comparison	*P* Values
Age			
STGD1	44 ± 15	STGD1 vs. STGD2	>0.05
STGD2	44 ± 19	STGD1 vs. Controls	>0.05
Controls	45 ± 17	STGD2 vs. Controls	>0.05
BCVA, logMAR			
STGD1	0.42 ± 0.28	STGD1 vs. STGD2	<0.01
STGD2	1.09 ± 0.36	STGD1 vs. Controls	<0.01
Controls	0.0 ± 0.0	STGD2 vs. Controls	<0.01
RNFL			
STGD1	98 ± 9	STGD1 vs. STGD2	>0.05
STGD2	98 ± 10	STGD1 vs. controls	<0.01
Controls	107 ± 10	STGD2 vs. Controls	<0.01
CMT			
STGD1	129 ± 58	STGD1 vs. STGD2	<0.01
STGD2	65 ± 48	STGD1 vs. Controls	<0.01
Controls	240 ± 11	STGD2 vs. Controls	<0.01
Full retinal thickness			
STGD1	248 ± 52	STGD1 vs. STGD2	<0.01
STGD2	189 ± 42	STGD1 vs. Controls	<0.01
Controls	403 ± 16	STGD2 vs. Controls	<0.01
CT			
STGD1	268 ± 92	STGD1 vs. STGD2	>0.05
STGD2	242 ± 99	STGD1 vs. controls	<0.05
Controls	322 ± 45	STGD2 vs. controls	<0.01
EZ-RPE			
STGD1	55 ± 19	STGD1 vs. STGD2	<0.01
STGD2	26 ± 13	STGD1 vs. controls	<0.01
Controls	73 ± 6	STGD2 vs. controls	<0.01
ONL			
STGD1	33 ± 12	STGD1 vs. STGD2	<0.01
STGD2	17 ± 15	STGD1 vs. controls	<0.01
Controls	93 ± 7	STGD2 vs. controls	<0.01
OPL			
STGD1	21 ± 12	STGD1 vs. STGD2	<0.01
STGD2	19 ± 7	STGD1 vs. controls	<0.01
Controls	42 ± 6	STGD2 vs. controls	<0.01
INL			
STGD1	37 ± 7	STGD1 vs. STGD2	<0.01
STGD2	27 ± 4	STGD1 vs. controls	<0.01
Controls	47 ± 6	STGD2 vs. controls	<0.01
IPL			
STGD1	39 ± 8	STGD1 vs. STGD2	<0.01
STGD2	27 ± 4	STGD1 vs. controls	<0.01
Controls	49 ± 7	STGD2 vs. controls	<0.01
GCL			
STGD1	50 ± 8	STGD1 vs. STGD2	<0.01
STGD2	34 ± 7	STGD1 vs. controls	<0.01
Controls	63 ± 7	STGD2 vs. controls	<0.01

Table 3. Continued

Parameter	Mean ± SD	Comparison	*P* Values
HF_retina			
STGD1	7 ± 7	STGD1 vs. STGD2	<0.05
STGD2	10 ± 7	STGD1 vs. controls	<0.01
Controls	0 ± 0	STGD2 vs. controls	<0.01
HF_choroid			
STGD1	11 ± 11	STGD1 vs. STGD2	<0.01
STGD2	30 ± 20	STGD1 vs. controls	<0.01
Controls	0 ± 0	STGD2 vs. controls	<0.01
VD mSCP			
STGD1	0.40 ± 0.02	STGD1 vs. STGD2	>0.05
STGD2	0.40 ± 0.02	STGD1 vs. controls	<0.01
Controls	0.41 ± 0.01	STGD2 vs. controls	<0.01
VD mDCP			
STGD1	0.26 ± 0.06	STGD1 vs. STGD2	>0.05
STGD2	0.28 ± 0.07	STGD1 vs. controls	<0.01
Controls	0.43 ± 0.01	STGD2 vs. controls	<0.01
VD mCC			
STGD1	0.42 ± 0.03	STGD1 vs. STGD2	<0.01
STGD2	0.17 ± 0.17	STGD1 vs. controls	<0.01
Controls	0.50 ± 0.01	STGD2 vs. controls	<0.01
VD RPC			
STGD1	0.42 ± 0.02	STGD1 vs. STGD2	>0.05
STGD2	0.42 ± 0.02	STGD1 vs. controls	<0.01
Controls	0.44 ± 0.01	STGD2 vs. controls	<0.01
VD nSCP			
STGD1	0.41 ± 0.03	STGD1 vs. STGD2	>0.05
STGD2	0.40 ± 0.04	STGD1 vs. controls	>0.05
Controls	0.43 ± 0.01	STGD2 vs. controls	<0.05
VD nDCP			
STGD1	0.30 ± 0.02	STGD1 vs. STGD2	>0.05
STGD2	0.30 ± 0.03	STGD1 vs. controls	<0.01
Controls	0.40 ± 0.02	STGD2 vs. controls	<0.01
VD nCC			
STGD1	0.50 ± 0.02	STGD1 vs. STGD2	<0.01
STGD2	0.52 ± 0.04	STGD1 vs. controls	<0.01
Controls	0.54 ± 0.03	STGD2 vs. controls	<0.01
VD mean			
STGD1	0.39 ± 0.01	STGD1 vs. STGD2	<0.01
STGD2	0.36 ± 0.03	STGD1 vs. controls	<0.01
Controls	0.45 ± 0.01	STGD2 vs. controls	<0.01
Vdisp mSCP			
STGD1	23.86 ± 6.43	STGD1 vs. STGD2	>0.05
STGD2	25.54 ± 11.83	STGD1 vs. controls	<0.01
Controls	10.53 ± 4.08	STGD2 vs. controls	<0.01
Vdisp mDCP			
STGD1	27.71 ± 9.61	STGD1 vs STGD2	>0.05
STGD2	26.50 ± 7.54	STGD1 vs. controls	<0.01
Controls	11.36 ± 3.50	STGD2 vs. controls	<0.01

Table 3. Continued

Parameter	Mean ± SD	Comparison	*P* Values
Vdisp RPC			
STGD1	26.71 ± 9.46	STGD1 vs. STGD2	<0.01
STGD2	20.62 ± 6.74	STGD1 vs. controls	<0.01
Controls	10.67 ± 3.75	STGD2 vs. controls	<0.01
Vdisp nSCP			
STGD1	28.41 ± 12.61	STGD1 vs. STGD2	<0.01
STGD2	20.40 ± 7.72	STGD1 vs. controls	<0.01
Controls	10.40 ± 2.92	STGD2 vs. controls	<0.01
Vdisp nDCP			
STGD1	28.37 ± 9.49	STGD1 vs. STGD2	>0.05
STGD2	24.75 ± 10.80	STGD1 vs. controls	<0.01
Controls	10.50 ± 3.34	STGD2 vs. controls	<0.01
VDisp mean			
STGD1	27.01 ± 6.58	STGD1 vs. STGD2	<0.05
STGD2	23.56 ± 5.61	STGD1 vs. controls	<0.01
Controls	10.69 ± 1.37	STGD2 vs. controls	<0.01
VT mSCP			
STGD1	5.39 ± 0.11	STGD1 vs. STGD2	>0.05
STGD2	5.27 ± 0.44	STGD1 vs. controls	<0.01
Controls	7.20 ± 0.31	STGD2 vs. controls	<0.01
VT mDCP			
STGD1	5.08 ± 0.31	STGD1 vs. STGD2	>0.05
STGD2	4.46 ± 0.84	STGD1 vs. controls	<0.01
Controls	7.85 ± 0.35	STGD2 vs. controls	<0.01
VT RPC			
STGD1	5.93 ± 0.30	STGD1 vs. STGD2	>0.05
STGD2	5.24 ± 0.66	STGD1 vs. controls	<0.01
Controls	7.73 ± 0.30	STGD2 vs. controls	<0.01
VT nSCP			
STGD1	4.49 ± 0.30	STGD1 vs. STGD2	>0.05
STGD2	4.56 ± 0.87	STGD1 vs. controls	<0.01
Controls	8.43 ± 0.33	STGD2 vs. controls	<0.01
VT nDCP			
STGD1	5.24 ± 0.30	STGD1 vs. STGD2	>0.05
STGD2	5.19 ± 0.42	STGD1 vs. controls	<0.01
Controls	7.07 ± 0.25	STGD2 vs. controls	<0.01
VT mean			
STGD1	5.23 ± 0.15	STGD1 vs. STGD2	<0.01
STGD2	4.94 ± 0.61	STGD1 vs. controls	<0.01
Controls	7.66 ± 0.23	STGD2 vs. controls	<0.01
VR mSCP			
STGD1	0.43 ± 0.02	STGD1 vs. STGD2	<0.01
STGD2	0.47 ± 0.03	STGD1 vs. controls	<0.01
Controls	0.39 ± 0.01	STGD2 vs. controls	<0.01
VR mDCP			
STGD1	0.45 ± 0.02	STGD1 vs. STGD2	<0.01
STGD2	0.50 ± 0.03	STGD1 vs. controls	<0.01
Controls	0.41 ± 0.01	STGD2 vs. controls	<0.01

Table 3. Continued

Parameter	Mean ± SD	Comparison	*P* Values
VR RPC			
STGD1	0.46 ± 0.01	STGD1 vs. STGD2	<0.01
STGD2	0.49 ± 0.01	STGD1 vs. controls	<0.01
Controls	0.44 ± 0.01	STGD2 vs. controls	<0.01
VR nSCP			
STGD1	0.49 ± 0.02	STGD1 vs. STGD2	<0.01
STGD2	0.48 ± 0.02	STGD1 vs. controls	<0.01
Controls	0.44 ± 0.01	STGD2 vs. controls	<0.01
VR nDCP			
STGD1	0.43 ± 0.02	STGD1 vs. STGD2	<0.01
STGD2	0.42 ± 0.02	STGD1 vs. controls	<0.01
Controls	0.40 ± 0.01	STGD2 vs. controls	<0.01
VR mean			
STGD1	0.45 ± 0.01	STGD1 vs. STGD2	<0.01
STGD2	0.47 ± 0.02	STGD1 vs. controls	<0.01
Controls	0.42 ± 0.01	STGD2 vs. controls	<0.01

patients' cohort into better and worse morphofunctional groups. Interestingly, STGD1 and STGD2 subgroups did not differ significantly in terms of foveal sparing, suggesting that other factors besides the atrophic changes of the fovea contribute to the BCVA loss. We hypothesize that the more extensively dysfunctional vascular network typical of STGD2 is responsible for an overall decrease in macular functionality. In other words, assuming the same degree of foveal involvement, a more trophic vascular network leads to a better retinal function. Although obtained from what is only a pilot study, our findings may have important clinical implications. In particular, patient evaluation in clinical practice might benefit from the information provided by this kind of analysis, enabling different clinical phenotypes to be identified. Furthermore, viewed in the context of clinical trials designed to test potential drugs, this approach might have a role in patient selection and in assessing clinical and anatomic outcomes.

Our study has undoubted limitations. Both OCT and OCTA analyses are known to be potentially affected by a number of artifacts,[14,15] so we adopted all possible precautions to minimize their potential effect on data analysis. We are also aware that our imaging-based analysis might certainly benefit from histopathologic validation. Last, our cases were insufficient to draw definitive conclusions and it would therefore be advisable to carry out a longitu-

dinal follow-up of patients in order to confirm our data.

In essence, our study reveals that extensive changes both in the retinal vascular network and in the retinal layers can be detected in STGD. A quantitative cutoff based on VT can separate two different morphofunctional phenotypes.

We believe a quantitative assessment might contribute to more accurate patients' categorization in a future scenario that sees possible new drugs combining with the introduction of artificial intelligence–based techniques to identify and treat STGD. Further studies are warranted to provide further support to the present findings.

Acknowledgments

Disclosure: **A. Arrigo**, None; **F. Romano**, None; **E. Aragona**, None; C. **di Nunzio**, None; **A. Sperti**, None; **F. Bandello**, Allergan Inc, Bayer Shering-Pharma, Hoffmann-La-Roche, NTC Pharma, Novartis, SIFI, SOOFT, Thrombogenics, Zeiss (C); **M. Battaglia Parodi**, None

References

1. Lu LJ, Liu J, Adelman RA. Novel therapeutics for Stargardt disease. *Graefes Arch Clin Exp Ophthalmol*. 2017;255:1057–1062.
2. Tanna P, Strauss RW, Fujinami K, Michaelides M. Stargardt disease: clinical features, molecular genetics, animal models and therapeutic options. *Br J Ophthalmol*. 2017;101:25–30.
3. Klufas MA, Tsu I, Sadda SR, Hosseini H, Schwartzm SD. Ultrawidefield autofluoresence in ABCA4 Stargardt disease. *Retina*. 2018;38: 403–415.
4. Pellegrini M, Acquistapace A, Oldani M, et al. Dark atrophy: an optical coherence tomography angiography study. *Ophthalmology*. 2016;123: 1879–1886.
5. Mastropasqua R, Toto L, Borrelli E, et al. Optical coherence tomography angiography findings in Stargardt disease. *PLoS One*. 2017;12: e0170343.
6. Battaglia Parodi M, Cicinelli MV, Rabiolo A, Pierro L, Bolognesi G, Bandello F. Vascular abnormalities in patients with Stargardt disease assessed with optical coherence tomography angiography. *Br J Ophthalmol*. 2017;101:780–785.
7. Invernizzi A, Pellegrini M, Acquistapace A, et al. Normative data for retinal-layer thickness maps generated by spectral-domain OCT in a white population. *Ophthalmol Retina*. 2018;2:808–815.
8. Van Huet RA, Bax NM, Westeneng-Van Haaften SC, et al. Foveal sparing in Stargardt disease. *Invest Ophthalmol Vis Sci*. 2014;55:7467–7478.
9. Arrigo A, Aragona E, Capone L, et al. Advanced optical coherence tomography angiography analysis of age-related macular degeneration complicated by onset of unilateral choroidal neovascularization. *Am J Ophthalmol*. 2018;195: 233–242.
10. Saint-Geniez M, Kurihara T, Sekiyama E, Maldonado AE, D'Amore PA. An essential role for RPE-derived soluble VEGF in the maintenance of the choriocapillaris. *Proc Natl Acad Sci U S A*. 2009;106:18751–18756.
11. Molday RS, Zhong M, Quazi F. The role of the photoreceptor ABC transporter ABCA4 in lipid transport and Stargardt macular degeneration. *Biochim Biophys Acta*. 2009;1791:573–583.
12. Battaglia Parodi M, Sacconi R, Romano F, Bandello F. Hyperreflective foci in Stargardt disease: 1-year follow-up. *Graefes Arch Clin Exp Ophthalmol*. 2019;257:41–48.
13. Battaglia Parodi M, Arrigo A, Romano F, et al. Hyperreflective foci number correlates with choroidal neovascularization activity in angioid streaks. *Invest Ophthalmol Vis Sci*. 2018;59: 3314–3319.
14. Spaide RF, Fujimoto JG, Waheed NK. Image artifacts in optical coherence tomography angiography. *Retina*. 2015;35:2163–2180.
15. Spaide RF, Fujimoto JG, Waheed NK, Sadda SR, Staurenghi G. Optical coherence tomography angiography. *Prog Retin Eye Res*. 2018;64:1–55.